Development of a Precision Scanning Optical Pulser for Low-Temperature Particle Detectors

Felix T. Jaeckel, Linh N. Le, Kyle W. Martin, and S. T. P. Boyd, Member *IEEE*

***Abstract*—Gamma-ray spectroscopy using low-temperature microcalorimeter arrays has demonstrated breakthrough energy resolution, establishing an important new technique for the precise characterization of radioactive samples. However, the pixels in these arrays must operate over an extraordinary dynamic range, with energy resolution of tens of eV over an energy range of hundreds of keV. Even small variations of the energy calibration from pixel to pixel can thus significantly reduce the effective energy resolution of the array relative to the energy resolution that may be achieved with a single pixel. The capability to measure microcalorimeter energy calibration with high precision over a wide dynamic range is required to evaluate and evolve future pixel designs and readout schemes to best meet these stringent requirements and facilitate further performance improvement. In this report we describe the design, development, and initial reflectivity-map testing of a new optical pulser intended for the precise determination of the energy calibration of microcalorimeter pixels and pixel arrays. 3K optics, in combination with a micron-resolution cryogenic XYZ scanner, enable forming and focusing of the light beam onto detectors mounted on the adiabatic demagnetization refrigerator, and permit scanning over detector area up to 20 mm x 20 mm. A beam splitter and photodiodes, also at 3 K, provide monitoring of both the incident and reflected beams, and absolute calibration of the absorbed power can be determined via a temperature difference and precision thermometry. Our initial measurements have demonstrated a focused spot size of 3 μm and the creation of high-resolution reflectivity maps of detectors, ensuring that energy can be deposited on the absorbers with high spatial precision even in the presence of differential thermal contraction and the compliance of the fiber suspension of the ADR.**

***Index Terms*—microcalorimeter, calibration, optical pulsing, position-dependence**

I. Introduction

MICROCALORIMETERS for gamma-ray spectroscopy have achieved energy resolution up to an order of magnitude better than conventional high-purity germanium (HPGe) detectors [1]-[5]. Because an individual microcalorimeter can provide only a small detector area and a low count rate, microcalorimeter gamma-ray spectrometers employ an array of individual microcalorimeter "pixels" to obtain an aggregate count rate and detector area roughly comparable to an HPGe detector. Hoteling *et al.* pointed out [6] that the move to increasingly large arrays of microcalorimeters increases the difficulty of maintaining the outstanding energy resolution that can be achieved with a single microcalorimeter across an entire array, due to complex calibration shapes and pixel-to-pixel variability of the individual superconducting transition-edge-sensor (TES) pixels.

One approach to improving this situation would be to develop microcalorimeter pixels with simpler calibration shapes and reduced pixel-to-pixel variability. Of particular interest in this context is the possibility of using pixels based on magnetic, rather than resistive, thermometry [7]. Our research group is working to develop magnetic microcalorimetry [8]-[11]. The energy resolution performance at 6 keV of a magnetic pixel using a sensor geometry our research group developed [8] has recently been shown by the Heidelberg group to be competitive with TES [13]. Work in magnetic gamma-ray pixels has been reported by the Loidl group in collaboration with the Heidelberg group [12] and testing of a prototype magnetic gamma-pixel was reported recently by the Heidelberg group [13].

Magnetic microcalorimeters offer potential advantages for array spectrometers because they rely on the measurement of an equilibrium thermodynamic property (magnetization) of a single-phase system, compared to TES devices, which measure a transport property (electrical resistance) in a mixed-phase system (at the superconducting transition). In general, we expect an equilibrium thermodynamic property in a single-phase system to be much less sensitive to impurity levels and fabrication process parameters. Further, the complications introduced by electrothermal feedback to the details of TES calibrations are absent from the magnetic approach. The magnetic approach should thus have both a simple physics-based calibration, as recommended in [6], and less pixel-to-pixel variability. Additional advantages to the magnetic approach may also result from the ease with which the heat capacity of the sensor can be tuned.

Our group is currently performing research to help determine whether or not the potential advantages of the magnetic pixel are borne out in practice. However, whether the best-performing pixels turn out to be TES or magnetic, or another approach entirely, a measurement system is needed to precisely determine calibration shape and pixel-to-pixel

Manuscript received October 9, 2012. This work was supported by the U.S. Department of Energy and the Defense Threat Reduction Agency.

Felix T. Jaeckel is with the Department of Physics and Astronomy, University of New Mexico, Albuquerque, NM 87131 USA (phone: 505-620-4876; fax: 505-277-1520; e-mail: jaeckel@unm.edu).

Linh N. Le is with the Department of Physics and Astronomy, University of New Mexico, Albuquerque, NM 87131 USA (e-mail: linhle@unm.edu).

Kyle W. Martin is with the Department of Physics and Astronomy, University of New Mexico, Albuquerque, NM 87131 USA (e-mail: kmartin1@unm.edu).

Stephen T. P. Boyd is with the Department of Physics and Astronomy, University of New Mexico, Albuquerque, NM 87131 USA (e-mail: stpboyd@unm.edu).

reproducibility of new candidate pixels.

Our approach to this problem is a precision scanning optical pulser. Delivery of well-controlled light pulses into cryostats via fiber optic is routinely performed in quantum optics experiments using cryogenic detectors [14]-[19], and the impact of black-body IR transmitted down the fiber from room temperature to the cold detector has recently been put on a semi-quantitative footing [20].

An optical pulser can easily achieve the large required dynamic range and precise control of the delivered light pulse energy. The ability to control and record the timing of delivered pulses and detector responses permits signal averaging for high precision. The use of a cryogenic XYZ scanner permits the use of cold focusing optics, allowing us to achieve a small spot size even with a 6 mm distance between the scanner (on the 3K stage) and the absorber (on the adiabatic demagnetization refrigerator (ADR) stage). The scanning range in the horizontal X and Y directions is large, 20 mm × 20 mm, allowing the study of multiple devices per cooldown or pixel arrays of significant size. The scanner positioning accuracy is ~1 μm. The combination of signal averaging, precise timing, small spot size, and precise spot positioning may also prove to be a useful new probe of the detailed dynamics of thermalization in the detectors.

However, along with these very strong qualifications for the job, the optical pulser also has two apparent weaknesses for microcalorimetry testing.

First, the energy deposition physics of a photon that can be delivered to an absorber by a fiber optic is quite different from that of an X- or γ-ray. However, the difference in the energy deposition physics is of little importance if our main goal is to determine pixel-to-pixel variability. It also seems unlikely that the difference in deposition physics will keep us from determining whether or not a new pixel design has a simple calibration shape. However, this assumption must be continuously scrutinized as the data-taking proceeds, as the difference in deposition physics will certainly impact the details of the calibration shape at some level.

The second apparent weakness of the pulser approach is that, at the wavelengths that can be easily delivered by an optical fiber, the reflectivity of the absorber is dependent on both absorber material and surface condition, so the ratio of deposited energy to applied energy will be a function of absorber material and the position of the focused spot on the absorber. We plan to determine this ratio with a thermal power measurement: at low temperatures the absolute power absorbed from the light beam can be determined by comparing the temperature rise or slope change caused by the beam to the temperature rise or slope change caused by an electrical resistance heater located on the same stage as the detector.

II. Design

A. Overview

The optical pulser uses a room-temperature light source for precise and flexible control of the generated pulses. The light source is coupled via optical fiber to the microcalorimeters under study, which are mounted in a pulse-tube cooled cryostat. Fig. 1 shows the pulser components on the 3K flange and the ADR.

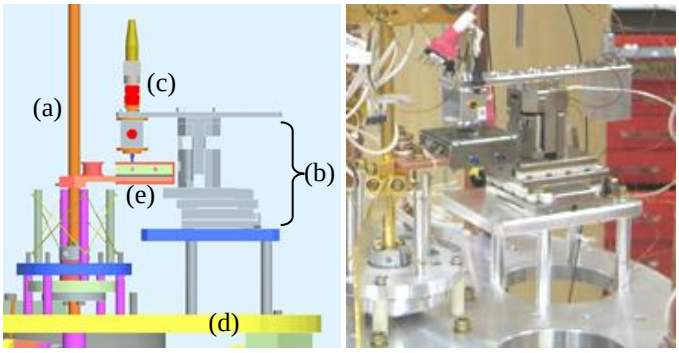

Fig. 1. The cold parts of the scanning pulser. Left: solid model view, showing: (a) vertical copper rod from the salt pill of the adiabatic demagnetization refrigerator, (b) XYZ scanning stage stack, (c) objective assembly, fiber optic connector shown at top, (d) 3 K flange, (e) shielded box holding detectors. Right: as implemented. A counterweight for the optical head reduces off-axis loading of the XYZ scanning stage.

Although for positioning stability we would prefer for both the scanner and the microcalorimeters to be strongly mechanically connected, the heat generated by the scanner (described further below) requires that it be mounted on the 3K flange of the cryostat, while the microcalorimeters must be mounted on the ADR stage.

The cold end of the fiber connects to the objective assembly mounted on the XYZ scanner. The objective assembly focuses the beam to a spot about 6mm distant from the housing of the last lens, and provides continuous *in-situ* monitoring of the power of both the incident and reflected beams.

The microcalorimeters are mounted on a stage attached to the ADR. In the measurements presented here, the microcalorimeters were housed in a shielded box with small windows to allow the focused spot to reach down to the components inside the shielded box while maintaining a minimum clearance of ~3mm between the objective assembly and the outside of the box.

The microcalorimeters used in these measurements have integral SQUIDs [8]-[11] which form the first stage of 2-stage SQUID amplification. The SQUID array amplifiers were mounted at 3 K. Initial pulse testing on prototype detectors is underway and will be described in a future report.

Further detail on each of the major components of the system is given in the subsections below.

B. Light-source

The pulser can be configured to work with any wavelength that can be delivered via fiber optic. For these measurements we chose to work with 405 nm light for several reasons.

To reduce the amount of stray light, low reflectance of the absorber is desired. While the reflectance of tin and bismuth is about ~0.7 and relatively constant over the visual spectrum, the reflectance of gold, which has been used as an absorber for magnetic pixels [7][13], decreases sharply below ~600 nm.

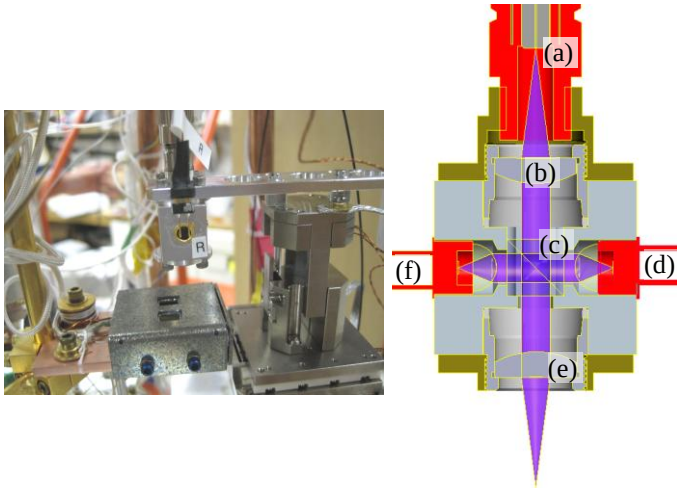

Fig. 2. Objective assembly. Left: detail of objective assembly in "stowed" position, well above the windows in the shielded box. Label "R" indicates photodiode measuring reflected light. Right: optical path inside the objective assembly. Light enters at top via fiber optic connection (a) and passes through the first aspheric lens (b) to form a collimated beam. The non-polarizing beam splitter (c) directs 50% of the beam to photodiode (d) for *in-situ* monitoring of the incident beam power. The remainder of the incident beam passes through the second aspheric lens (e) to focus on the detector. Reflected light is collimated by the same lens (e) and passes through the beam splitter (c) to photodiode (f) to monitor the reflected beam power. For the initial work reported here lenses (b) and (e) were selected for a long focal length of 10.6 mm, but they can easily be swapped out for a shorter focal length to achieve a smaller spot size, at the cost of reducing the working distance.

Shorter wavelength also enables us to obtain smaller spot-sizes and permits more aggressive IR filtering. We therefore decided on using a 405 nm (Blu-ray) laser diode. Keeping the selected wavelength in the visible regime also allows for visual assessment of local reflectivity variations over the absorber area using a microscope.

A potential disadvantage of using a shorter wavelength is that fewer photons are required to make up a pulse of a given energy. For a single pulse of 100 keV, a lower bound on the energy uncertainty of 0.55%=550 eV is set by Poisson statistics of the 405 nm (3 eV) photons. However, signal averaging removes this limit.

The laser diode is coupled into a single mode fiber with a free-space optical fiber coupler [21]. Free-space coupling allows us to easily insert and remove attenuators into and from the beam. A commercial laser diode driver [22] is used in constant-current mode and offers a modulation bandwidth of 2 MHz.

For good stability of the output power and wavelength, the laser diode is thermally stabilized using a thermoelectric-cooler and thermistor readout [21]. We have demonstrated temperature stabilities of about 0.4 mK over a 12 hour period, and fiber-coupled optical power stable to about 0.3% for a pig-tailed laser diode.

C. *Objective Assembly*

The objective assembly is shown in Fig. 2. While it would be possible to obtain a small spot size by bringing the fiber into close proximity with the sample, we have chosen instead to build a cold microscope objective to focus the output of the fiber onto the sample. This approach allows us to launch the beam across a macroscopic gap (~few mm) between the 3K components of the pulser and the components mounted on the ADR. This reduces the risk of damaging the fiber or the sample, especially in those cases were severe topography is present due the thick absorbers required for gamma-ray calorimeters. As shown in Fig. 2, incident and reflected beam power are monitored *in-situ* by photodiodes that can operate at low temperatures (Hamamatsu S2386-18L [23]. The entire assembly, shown in Fig. 2, is small and lightweight enough to be supported from a beam on the XYZ stage with a balancing counterweight.

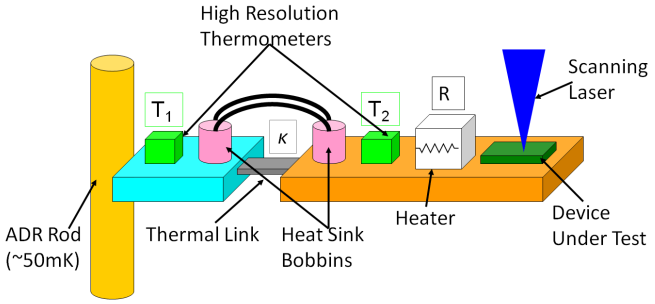

Fig. 3. Measuring absorbed power via thermometry. See text for details.

D. *Scanner*

For reliable and precise 3-axis positioning at low temperatures, a stack of three commercial single-axis stick-slip positioners [24] were chosen. The focusing axis is vertical (Z) and has travel of 12 mm. Only a small fraction of that 12 mm is required for focusing, so the pulser can in principle accommodate significant topography. The identical X and Y axes each have travel of 20 mm. All 3 axes are equipped with resistive position readout for closed-loop position control, which provides μm-resolution and repeatability in positioning. The 20 mm x 20 mm horizontal range of travel provides sufficient room to test several devices or a microcalorimeter array of significant size.

Each of the three stages in the XYZ scanner generates heat due to both the resistive position readout (est. 2 mW per stage) and in proportion to their velocity, from both mechanical and electrical dissipation (total est. ~19 mW for 0.1mm/s). Because of these heating levels the scanner stack is supported on the lower 3K flange in our system. A steady-state temperature rise of about 0.1 K is observed on that flange for continuous scanning at speed of 0.1 mm/s.

E. *Absorbed Power Measurement*

Accurate comparison of the response of two pixels, or of a single pixel with itself when it is stimulated at different locations on the absorber, requires accurate knowledge of the absorbed energy. Because our monitor of reflected power only measures that part of the light that reflects back into the objective assembly optics, absorber surface roughness and misalignment will generally make it impossible to deduce absorbed power only from knowledge of incident and reflected power. However, we can determine the absorbed power by measuring temperatures. Fig. 3 shows a schematic of the new microcalorimeter stage being constructed for the

next round of pulser measurements. By installing the detectors on a stage connected to the ADR through a thermal link of known conductance, absorbed power can be deduced by comparing the change in the temperature difference across the conductance that results from the optical beam to the change that results from supplying an electrical resistance heater on the detector stage with known power. The miniature "high resolution thermometers" indicated in Fig. 3 are in fact just simple modifications to our magnetic microcalorimeter designs.

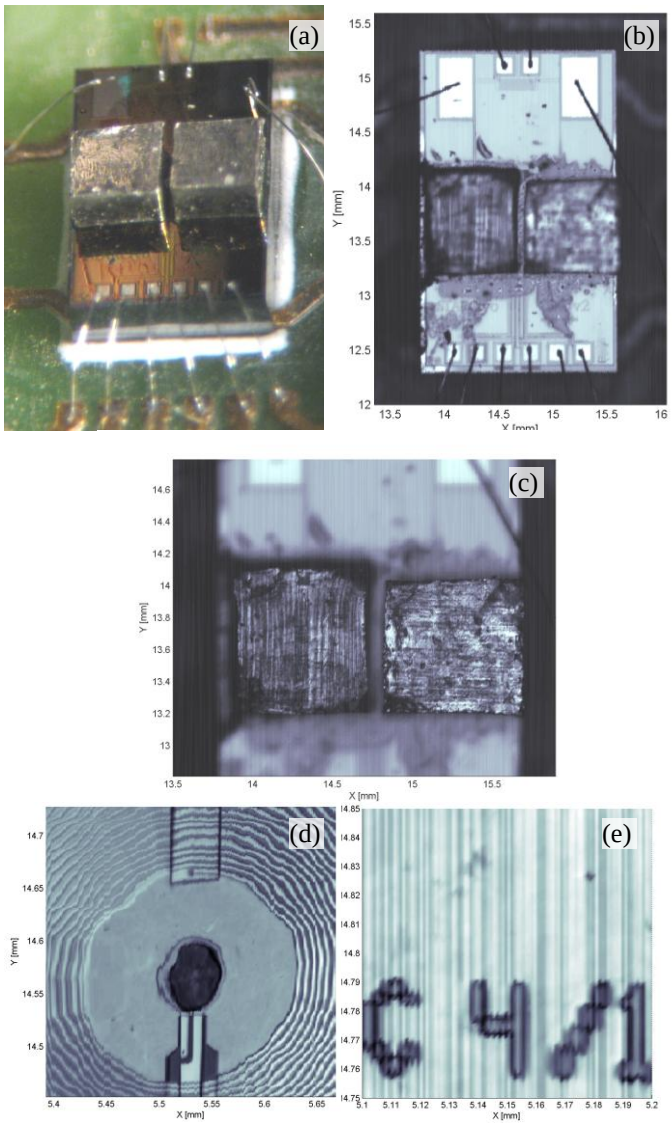

Fig. 4. An optical micrograph, taken at room temperature, and some example reflectance scans taken at low temperature with the new scanning pulser. (a) optical micrograph taken after this prototype device was bonded. The die is 2×3 mm, and the tin absorber blocks are nominally 0.8×0.8×0.5 mm. (b) reflectivity scan at 1.3K made with 9 × 9 μm pixels, with focus set on the surface of the die. Clearly visible are the wire-bonds to the SQUID bond-pads at the bottom and the excitation coil persistence switch bond pads near the top. Variation in the size of the tin blocks on this prototype device is clearly apparent, as well as residual adhesive on the die surface that was not obvious under optical microscopy. (c) reflectivity scan at 1.3K with 6×6 μm pixels, with focus set on the top surfaces of the tin blocks. (d) impact of differential thermal expansion on high-resolution scans. This 1×1 μm pixel reflectivity scan on a different device in the same cooldown shows a 50μm-diameter × 1μm thick dot of sputtered Au:Er centered in the pickup loop of one of our miniature SQUID micro-susceptometer devices. The surrounding spiral is the magnetizing coil. Although the local resolution of this image is quite good, easily resolving the 2 μm spacing between the turns of the spiral coil, this scan was taken while the cryostat was being warmed up, causing the distortion. (e) another high-resolution scan with 1×1 μm pixels, taken on the same device but under equilibrated temperature conditions. The vertical striping in this image was an artifact of the early data-taking procedures and has since been eliminated. The smallest gap between the "/" and the "1" is about 4 μm and is clearly resolved. This scan demonstrates the precision with which a light pulse can be positioned.

III. Reflectance Scans

The principal new measurements obtained in this initial series of measurements are the reflectance scans, summarized in Fig. 4. These grayscale images show the ratio of the reflected and incident beams, measured *in-situ* by the photodiodes in the objective assembly. The ratio is taken to eliminate any impact from the output power variation of the diode laser. Bright regions correspond to maximum reflected light, dark regions to minimum reflected light. Images (a)-(c) are of one device, and images (d) and (e) are of another device from the same cooldown of the pulser.

In aggregate, the reflectance scan data obtained show that the cold focusing optics are working well, and that good focus can be found. The focused spot size is small and agrees with the calculated estimate of 3 μm. The beam positioning is precise and reproducible on the 1 μm scale.

IV. Summary

We have described the design, development, and initial testing of a new scanning optical pulser stage for the precise characterization of gamma-ray microcalorimeter pixels. Reflectivity scans demonstrate outstanding optical performance with optical resolution less than 3 μm and beam positioning to 1 μm. Continuous *in-situ* monitoring of incident and reflected beam power at the cold optics allow the creation of high-quality reflectivity scans at low temperature that permit extremely accurate beam placement in spite of the unavoidable misalignment that results from differential thermal contraction. This combination of capabilities, combined further with the timing information that an optical pulser can provide, should also advance the capabilities of the field for probing the position-dependent response of absorbers and the details of thermalization processes in microcalorimeters. Real-world pile-up testing can be targeted with full control over pulse timing to evaluate the performance of pulse processing algorithms. Initial testing of the pulsing capabilities of the scanner, using prototype devices, is currently underway.

Acknowledgments

The precision optical pulser project is supported principally by the U.S. Department of Energy (NA-22). We are also grateful to the Defense Threat Reduction Agency for the funds to procure the scanning stage. The authors also thank Alexander Albrecht for his help in setting up some of the optical assemblies.

REFERENCES

[1] A. S. Hoover, N. Hoteling, M. W. Rabin, J. N. Ullom, D. A. Bennett, P. J. Karpius, D. T. Vo, W. B. Doriese, G. C. Hilton, R. D. Horansky, K. D. Irwin, V. Kotsubo, D. W. Lee, L. R. Vale, "Large microcalorimeter arrays for high-resolution X- and gamma-ray spectroscopy," *Nuclear Inst. and Meth. in Phys. Research A*, vol. 652, pp. 302-305 (2011)

[2] A.S. Hoover, M.K. Bacrania, N.J. Hoteling, P.J. Karpius, M.W. Rabin, C.R. Rudy, D.T. Vo, J.A. Beall, D.A. Bennett, W.B. Doriese, G.C. Hilton, R.D. Horansky, K.D. Irwin, J.N. Ullom, L.R. Vale, "Microcalorimeter arrays for ultra-high energy resolution X- and gamma-ray detection," *Journal of Radioanalytical and Nuclear Chemistry*, vol. 282, pp. 227-232 (2009)

[3] M.K. Bacrania, A.S. Hoover, P.J. Karpius, M.W. Rabin, C.R. Rudy, D.T. Vo, J.A. Beall, D.A. Bennett, W.B. Doriese, G.C. Hilton, R.D. Horansky, K.D. Irwin, N. Jethava, E. Sassi, J.N. Ullom, L.R. Vale, "Large-Area Microcalorimeter Detectors for Ultra-High-Resolution X-Ray and Gamma-Ray Spectroscopy," *IEEE Transactions on Nuclear Science*, vol. 56, pp. 2299-2302 (2009)

[4] W.B. Doriese, J.N. Ullom, J.A. Beall, W.D. Duncan, L. Ferreira, G.C. Hilton, R.D. Horansky, K.D. Irwin, J.A.B. Mates, C.D. Reintsema, L.R. Vale, Y. Xu, B.L. Zink, M.W. Rabin, A.S. Hoover, C.R. Rudy, D.T. Vo, "14-pixel, multiplexed array of gamma-ray microcalorimeters with 47 eV energy resolution at 103 keV," Applied Physics Letters, vol. 90, pp. 193508 (2007)

[5] S. Friedrich, "Nuclear diagnostics with cryogenic spectrometers," Nuclear Instruments and Methods in Physics Research A, vol. 579, pp. 157-160 (2007)

[6] N. Hoteling, M. K. Bacrania, A. S. Hoover, M. W. Rabin, M. Croce, P. J. Karpius, J. N. Ullom, D. A. Bennett, R. D. Horansky, L. R. Vale, and W. B. Doriese "Issues in energy calibration, nonlinearity, and signal processing for gamma-ray microcalorimeter detectors," *AIP Conf. Proc.* 1185, 711 (2009)

[7] An excellent review of magnetic microcalorimetry as of 2005 is provided in A. Fleischmann, C. Enss, G.M. Seidel, "Metallic magnetic calorimeters," in *Cryogenic Particle Detection*: Springer-Verlag, Berlin: pp. 151-216 (2005).

[8] S. T. P. Boyd, R. H. Cantor, "Microcalorimeter magnetic sensor geometries using superconducting elements" (849.63 Kb), *AIP Conf. Proc.*, vol. 1185, pp. 595 (2009)

[9] S. T. P. Boyd, V. Kotsubo, R. H. Cantor, "Miniature thin-film SQUID susceptometer for magnetic microcalorimetry and thermometry," *IEEE Trans. Appl. Super.*, vol. 19, pp. 697-701 (2009)

[10] S.T.P. Boyd, R. Cantor, V. Kotsubo, P. Blumenfeld, J.A. Hall, "Characterization of a miniature thin-film SQUID susceptometer for metallic magnetic microcalorimetry," *J. Low Temp. Phys.*, vol. 151, pp. 369 (2008).

[11] Robin Cantor, J. Ad Hall, Phil Blumenfeld, and Stephen T. P. Boyd, "Miniature thin-film superconducting quantum interference device susceptometer," *IEEE Trans. Appl. Super*, vol. 17, pp. 738 (2007).

[12] M. Rodrigues, A. Pabinger, S. Lausberg, M. Loidl, B. Censier, J. Bouchard, L. Fleischmann, A. Fleischmann, C. Enss, "Metallic magnetic calorimeters for gamma-ray spectrometry," *AIP Conf. Proc.*, vol. 1185, pp. 583-586 (2009).

[13] C. Pies, S. Schafer, S. Heuser, S. Kempf, A. Pabinger, J.-P. Porst, P Ranitsch, N. Foerster, D. Hengstler, A. Kampkotter, T. Wolf, L. Gastaldo, A. Fleischmann, C. Enss, "maXs: microcalorimeter arrays for high-resolution x-ray spectroscopy at GSI/FAIR", *J. Low Temp. Phys.* vol. 167, pp. 269-279 (2012).

[14] A. J. Miller, S. W. Nam, J. M. Martinis and A. V. Sergienko, "Demonstration of a low-noise near-infrared photon counter with multiphoton discrimination," *Appl. Phys. Lett.*, vol. 83, no. 4, pp. 791-793, Jul. 2003

[15] D. Rosenberg, A. E. Lita, A. J. Miller, and S. W. Nam, "Noise-free high-efficiency photon-number-resolving detectors," *Phys. Rev. A.*, vol. 71, p.061803, Jun. 2005

[16] A. E. Lita, A. J. Miller, and S. W. Nam, "Counting near-infrared singlephotons with 95% efficiency," *Opt. Express*, vol. 16, pp. 3032–3040, Mar. 2008

[17] D. Fukuda, G. Fujii, A. Yoshizawa, and H. Tsuchida, "High speed photon number resolving detector with titanium transition edge sensor," *J. Low Temp. Phys.*, vol. 151, pp. 100–105, Jan. 2008.

[18] D. Fukada, *et al.*, "Titanium-based transition-edge photon number resolving detector with 98% detection efficiency with index-matched small-gap fiber coupling," *Opt. Express*, vol. 19, no. 2, pp. 870-875, Jan. 2011

[19] W. H. P. Pernice, C. Schuck, O. Minaeva, M. Li, G. N. Goltsman, A. V. Sergienko and H. X. Tang, "High Speed and High Efficiency Travelling Wave Single-Photon Detectors Embedded in Nanophotonic Circuits," *arXiv:1108.5299v2*, Apr. 2012

[20] A. J. Miller, A. Lita, D. Rosenberg, S. Gruber, S. Nam, "Superconducting photon number resolving detectors: performance and promise," Proceedings of the 8th International Conference on Quantum Communication, Measurement and Computing, J. O. Hirota, H. Shapiro and M. Sasaki, Eds., (NICT Press, Japan, 2007), pp. 445-450.

[21] Thorlabs, 56 Sparta Avenue, Newton, NJ 07860. http://thorlabs.com

[22] Wavelength Electronics, 51 Evergreen Dr., Bozeman, MT 59715. http://www.teamwavelength.com

[23] Guy Michel, Kjetil Dohlen, Jerome Martignac, Jean-Claude Lecullier, Patrick Levacher, and Claude Colin, "Interferential scanning grating position sensor operating in space at 4 K," *Applied Optics*, vol. 42, pp. 6305-6313, Nov. 2003

[24] Attocube Systems AG, Königinstrasse 11a RGB, 80539 Munich, Germany. http://attocube.com.